Rock Mech Rock Eng (2015) 48:1207–1220
DOI 10.1007/s00603-014-0614-9

ORIGINAL PAPER

# Determination and Assessment of Parameters Influencing Rock Mass Cavability in Block Caving Mines Using the Probabilistic Rock Engineering System

Ramin Rafiee · Mohammad Ataei · Reza Khalokakaie · Seyed Mohammad Esmaeil Jalali · Farhang Sereshki

Received: 21 January 2014 / Accepted: 22 May 2014 / Published online: 10 June 2014


**Abstract** Mining methods such as block caving or sub-level caving rely on the characteristics of the rock mass to cave efficiently to fulfill an economical production. The identification of influencing parameters and cavability assessment are, thus, a prime geotechnical focus for all potential caving projects. In the caving operation, many factors, such as natural and induced factors, affect the caving performance. In this study, after discussing the caving process and identifying all effective parameters, the interaction matrix based on the rock engineering system (RES) is introduced to study the influencing parameters in rock mass cavability. The interaction matrix analyzes the interrelationship between the parameters affecting rock engineering activities. As the interaction matrix codes are not unique, probabilistic coding can be performed non-deterministically, allowing consideration of uncertainties in the RES analysis. As a result, the parameters with the highest probability of being dominant or subordinate, and also the parameters with the highest probability of being interactive, are introduced. The proposed approach could be a simple but efficient tool in the evaluation of the parameters affecting the cavability of rock mass in block caving mines and, hence, useful in decision-making under uncertainties.

**Keywords** Cavability of rock mass · Rock engineering system (RES) · Probabilistic coding

R. Rafiee (✉) · M. Ataei · R. Khalokakaie ·
S. M. E. Jalali · F. Sereshki
Shahrood University of Technology, Shahrood, Islamic Republic of Iran
e-mail: raminlamezi@gmail.com

## 1 Introduction

Block caving is an underground mass production system of ore extraction, which, under favorable conditions, has lower mining costs than any other underground method. Additional necessary features for block caving are a well-developed fracture system within the orebody and a capping material that is weak enough to cave along with the orebody (Julian 1974). Cavability refers to the capability of an in situ rock mass to unravel when undercut, and considers all three stages of caving: initiation, propagation, and continuous caving. Once the undercut has been blasted and removed, the ore column is unsupported from below and, if a failure or collapse of the cave back occurs, then the cave initiation has been achieved (Mawdesley 2002).

Predicting the cavability of a rock mass is an important issue in block cave design (Lorig et al. 1995). The reliable prediction of cavability is critical in determining the undercut dimensions required to initiate and continuously cave an orebody. The cavability of the rock mass will affect mine design and economic issues for a given geological environment, and is a fundamental issue in establishing a successful block caving mine. The cavability and resulting fragmentation of the ore zone, host rock, and cap rock must be determined when evaluating the applicability of block caving as a mining method (Mawdesley et al. 2001). Many researchers have attempted to assess the rock mass cavability. The earliest reported empirical system for predicting cavability was the cavability characterization of the Climax orebody based on rock type, fracture spacing, and mineralization (Mahtab and Dixon 1976). In later years, several parameters, including the rock quality designation (RQD) and powder factor for secondary blasting, were related to ore cavability to define a cavability index (CI), which represented the ease of caving (Obert et al.

1976). The application of Barton's $Q$-value as a predictor of cavability was first raised by White (1977). McMahon developed a CI based on the caving experience from the Climax and Urad mines, to predict the cavability, fragmentation, and secondary blasting requirements based on the RQD value. Laubscher's caving chart (Diering and Laubscher 1987; Laubscher 1990, 1994, 2000b) is the general industry standard method of assessing cavability mass based on the hydraulic radius and modified rock mass rating (MRMR) value. In this method, the precise form of the caving boundary on the caving chart for MRMRs greater than 50 was not known due to the limited caving experience for rock masses with higher MRMR values. Finally, the extended Mathews' stability graph based on logistic regression was proposed by Mawdesley (2002). In all those methods, the authors did not consider all the parameters and their interactions completely.

The rock engineering system (RES) is one of the most powerful approaches in rock engineering, which was first introduced by Hudson in 1992 to deal with complex engineering problems, as it combines adaptability, comprehensiveness, repeatability, efficiency, and effectiveness (Hudson and Harrison 1992; Jiao and Hudson 1995, 1998). In this approach, the main factors are arranged along the main diagonal elements of a matrix, a so-called interaction matrix, and the interrelations between pairs of factors are identified in off-diagonal elements. Many researchers have attempted to develop this method in various fields of rock mechanics, such as Shang et al. (2000), Zhang et al. (2004), Rozos et al. (2008), Budetta et al. (2008), Younessi and Rasouli (2010), and Zare Naghadehi et al. (2013).

There are several techniques for coding the interaction matrix in the RES method. One of the most often used techniques is the "expert semi-quantitative" (ESQ) coding method, in which only one value is deterministically assigned to each interaction. Hence, in this method, no uncertainties are considered in coding the interaction matrix. To overcome this problem, a probabilistic ESQ (PESQ) approach is proposed by Naghadehi et al. (2011). In this approach, the probabilities considered for each possible coding value address the uncertainties in the coding of the interaction matrix.

In this study using the PESQ method, the parameters with the highest probability of being dominant or subordinate, and also the parameters with the highest probability of being interactive in rock mass cavability, are found.

## 2 Rock Mass Cavability

The cavability of a deposit defines the ability of the orebody and overlying rock mass to cave freely and spontaneously, once undercut to a sufficient dimension.

The cavability of orebodies is important to various mining methods from different aspects. The block caving mining method relies on caving to extract massive ore economically, whereas other methods rely on the stability of the orebody and host rock to extract ore selectively. Block caving methods require more developments before the start of production than most other methods. Therefore, they have comparatively high initial capital costs and are relatively inflexible. If the cavability of the orebody is not determined with adequate accuracy, expensive and time-consuming measures may subsequently be required in order to initiate or sustain caving (van As and Jeffrey 2000).

The monitoring of many caving operations has shown that two types of caving can occur: stress caving and subsidence caving. The caving mechanism depends on the relations between the strength of the rock mass, the induced stresses, and the geometry and strengths of the discontinuities in the rock mass. Stress caving occurs when the induced stresses in the cave back exceed the strength of the rock mass, causing yielding and fragmentation of the rock mass into a caved rock state. Under these circumstances, the dominant mechanism of failure is brittle fracture of the intact rock (Heslop and Laubscher 1981).

Subsidence caving is characterized by low mining-induced stresses and is often analyzed by knowledge of the joint fabric and simple kinematics. Gravity-induced unraveling is expected to occur in the cave back (roof) as a tensile failure mechanism under low-stress conditions. Failure can occur through slip along pre-existing joints as the rock is unconfined from below, or through bending/deflection of the rock layers. Subsidence caving usually results in coarser drawpoint fragmentation, since a little damage is induced to the rock mass during its mobilization. Primary fragmentation in this case is usually close to the in situ block size.

## 3 Factors Influencing Cavability

The cavability of a deposit is a function of natural factors such as the geomechanical properties of the rock mass and mining-induced factors. Pre-mining stresses and rock mass properties fall into the category of natural factors, whilst induced stresses and mining-related effects are induced factors which influence cavability. In Fig. 1, the main factors affecting the cavability of a rock mass are shown.

### 3.1 Natural Factors

A host of geologic, geometric, and physical parameters are recognized to contribute to the cavability of a rock mass in a block cave (Kendorski 1978).

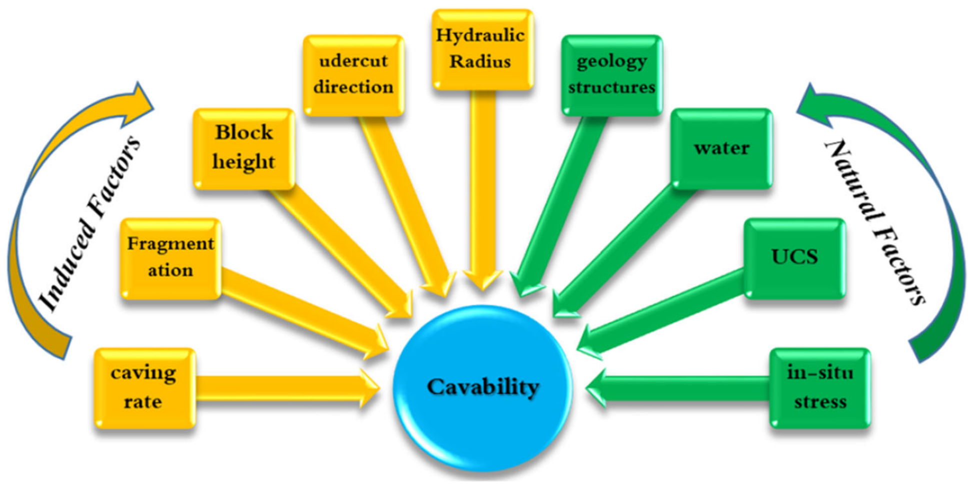


**Fig. 1** The main factors affecting the cavability of a rock mass

### *3.1.1 Geology Structures*

Fractures with a low shear resistance, favorable incline, and close spacing are important for caving an orebody (Mahtab and Dixon 1976). The determination of discontinuities orientation is one of the most important issues in cavability assessment. The orientation of the in situ stresses with respect to the orientation of the main discontinuity sets is an important consideration in determining the effectiveness of arching and locking-in of rock blocks (Kendorski 1978). Several sets of fractures are essential to develop a good caving. Low-angle structures lead to a suitable vertical displacement in the rock mass during the mining operation. They can accommodate both shear and gravity failure (Laubscher 2000b). A combination of one low-angle (0° to 30° dip) set of fractures and another nearly vertical (75° to 90° dip) set of fractures is the most effective two-dimensional fracturing configuration for ease of cavability of an orebody. In an actual three-dimensional situation, one set of low-angle fractures and two sets of nearly vertical fractures will be the most effective in improving the cavability. These observations, concerning favorable joint orientations, may be valid for environments lacking lateral confinement (Mahtab and Dixon 1976). Based on the simplistic cave demonstration models presented in Fig. 2, the following conclusions can be made:

- Joints that are orientated perpendicular to the direction of draw (i.e., in most cases, horizontal joints) are favorable for cave propagation. The mobilized zone advances vertically at the most rapid rate. In this case, the rate at which the mobilized zone progresses far exceeds the production draw rate.
- Joints that are orientated parallel to the direction of draw (i.e., in most cases, vertical joints) are not favorable for cave propagation. Minimal displacement of the rock mass is achieved above the mining footprint.
- Joints that are orientated at an angle to the direction of draw result in a preferred cave propagation direction.

Filling and persistence of discontinuities have a bearing on the cavability of the rock mass because these properties have an important role in the strength of rock mass. Such properties should be accurately measured by detailed scanline mapping and considered when assessing the cavability.

### *3.1.2 In Situ Stress Regime and Direction*

The orientation and magnitude of the in situ stress field can influence rock mass cavability. The ratio of the in situ horizontal to vertical stresses will affect the magnitude of the stresses induced in the cave back as caving initiates and will, in association with joint orientation, strongly influence cave propagation and the caving rate.

The orientation of a rectangular mining block with respect to the in situ principal stress direction has an effect on the cavability of rock mass. It is now understood that the redistribution of the maximum principal stress over a shorter footprint axis will promote cave propagation, since the cave back experiences greater stress concentrations when the maximum principal stress hits the cave "broadside" as opposed to "end-on". In the case of "end-on", the cave presents a larger obstacle to stress (Sainsbury 2012). The concept is presented in Fig. 3.

High confining stress may limit the cave initiation and propagation, despite favorable structure and geomechanical properties of the rock mass (Brady and Brown 2004). High horizontal stress can make the blocks interlocked and stabilize the rock mass against cave propagation in the absence of low-angled discontinuities within the rock mass (Kendorski 1978).

The amount and direction of in situ stress can affect the direction and dimension of undercut, fragmentation of rock

Fig. 2 Cave scale model results for varying joint orientations (Sainsbury 2012)

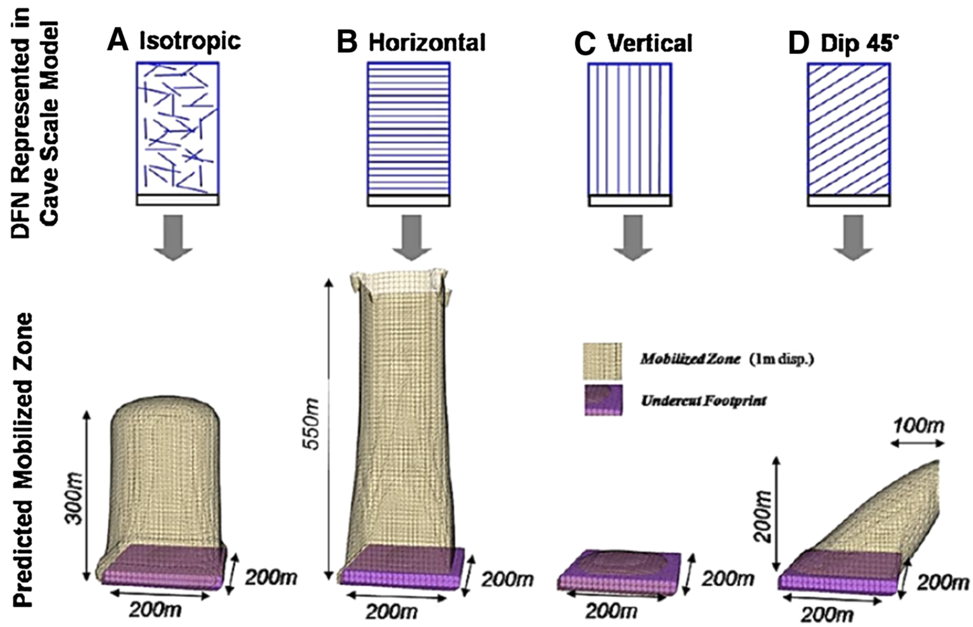


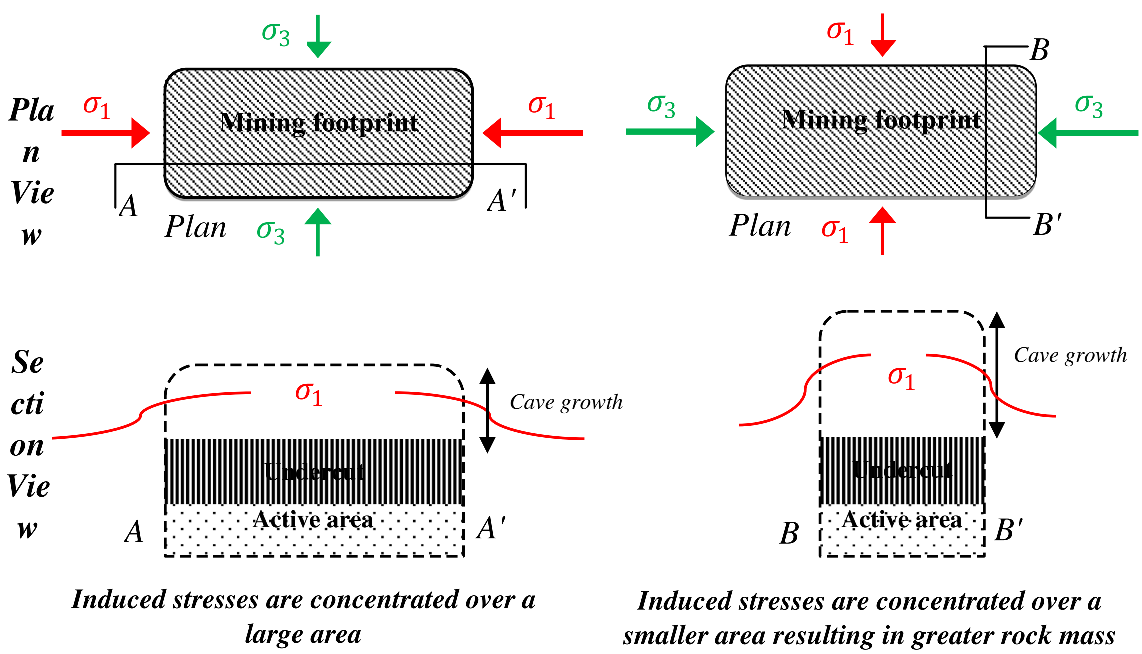


Fig. 3 Conceptual diagram of the effect of the principal stress direction on cavability (Sainsbury 2012)

mass, caving rate, and the geometry and strength properties of discontinuity.

### 3.1.3 Uniaxial Compressive Strength (UCS)

The compressive strength can be considered as the most widely used and quoted rock engineering parameter. The strength of rock is used as an important parameter in many rock classification systems, such as the rock mass rating (RMR) and the MRMR. The uniaxial compressive strength (UCS) is influenced by many rock characteristics, such as weathering or alteration rate, microcracks and internal fractures, density, and porosity. It is clear that the cavability of rock mass decreases when the strength of rock mass increases.

### 3.1.4 Water

Surface and groundwater management is of little concern in some caving operations, but it is vitally important in others. It is, therefore, necessary to consider issues such as the location of surface water paths and storages and rainwater drainage. Water in the potential cave zone can assist caving by reducing the friction on joints or by the effect of increased pore water pressure. The source of water can be ground water or water introduced during the rainy seasons.

## 3.2 Induced Factors

Although the cavability of orebody is a function of natural properties of rock mass, it is also significantly affected by induced factors. Induced parameters are a function of engineering decisions based on how the orebody is mined. The induced factors are not directly related to the natural properties or the immediate geomechanical characteristics of a particular orebody. However, the undercut geometry and sequence can be designed to take advantage of geotechnical domains and natural variability within the rock mass to cave for a reduced undercut area.

### *3.2.1 Block Height*

The block height depends on the geometry of the ore, and fragmentation and properties of the cap rock. The vertical distance between mining levels will affect the rock mass cavability (Kendorski 1978). Secondary fragmentation of caving material occurs through attrition as the ore is drawn down through the column. Thus, the cavability of ore, cap rock, and the result of fragmentation influence the determination of the optimal block height.

### *3.2.2 Undercut Condition*

The undercut extraction strategy can influence the cavability of a rock mass through the magnitude of the induced stresses developed in the cave back. Regarding the nature and importance of undercutting, Butcher (2000) has suggested that undercutting has three aims:

- To extract a void of sufficient dimensions to allow caving to occur;
- To achieve the required undercut dimension to initiate caving with minimum damage to the surrounding rock mass;
- To advance to caving hydraulic radius, initiate caving, propagate the cave, and, consequently, reduce the undercut abutment stress.

The choice of the starting or initiation point for the undercut and the preferred direction of undercut advance can be influenced by several factors, including (Laubscher 2003):

- The shape of the orebody,
- The distribution of grades within the orebody,

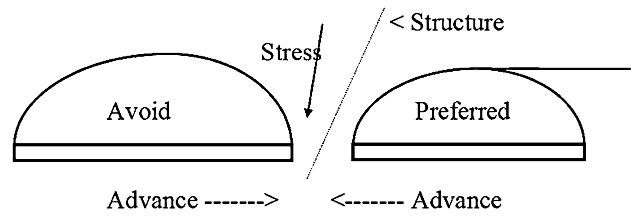


**Fig. 4** Favorable and unfavorable undercut directions (Laubscher 2000a)

- The in situ stress directions and magnitudes,
- The strength of the orebody and its spatial variation,
- The presence and orientations of major structural features in the orebody,
- The presence of caved areas adjacent to the block or panel to be undercut.

The direction of undercut developing into the principal stress direction will influence the magnitude of abutment stresses. Therefore, to reduce clamping stresses in the cave back, the undercuts are usually extracted in the direction of the maximum principal stress (Laubscher 2000b).

In the San Manuel mine, advancing an undercut from weak to strong rock led to caving problems and coarse fragmentation; however, when the undercut direction was changed from strong to weak rock, caving did occur and the fragmentation improved (Laubscher 2003).

If possible, the undercut direction should not be advanced towards structures that could initiate massive wedge failures, as shown in Fig. 4.

### *3.2.3 Hydraulic Radius*

The hydraulic radius is derived by dividing the area by the perimeter. The hydraulic radius influences the levels of stress induced on the extraction level. If the hydraulic radius is larger, the cave rating increases and develops more fractures and discontinuities. To propagate the cave, the hydraulic radius must be chosen based on the highest MRMR. The minimum span is considered by the hydraulic radius, as can be seen in Fig. 5, which shows how the hydraulic radius will vary for the same area if the minimum span is decreased.

### *3.2.4 Caving Rate*

The rate of upward advance of the yield zone is known as the "caving rate". Block caving is a low-selectivity mining method, and the caving rate is the only means of delaying dilution ingress into the broken ore in the cave. The control of the caving rate significantly affects the caving and fragmentation behavior (Brady and Brown 2004). The caving rate influences the rock mass quality, induced stresses, and the rate of development joints.

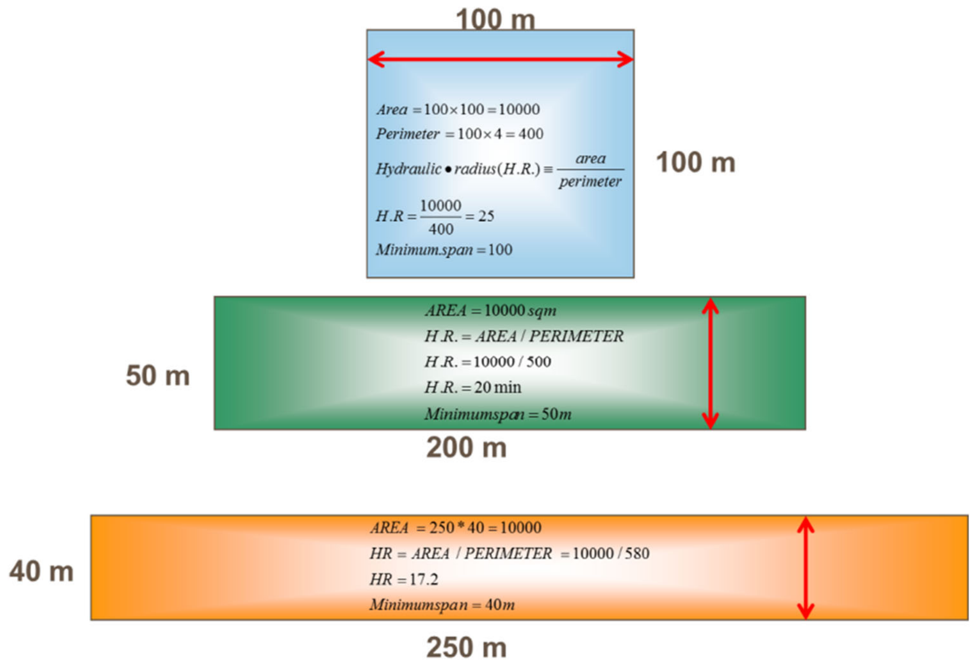


**Fig. 5** Undercut plan areas illustrating how the hydraulic radius reflects changes in the minimum span (Laubscher 2000b)

The rate of caving can be increased by advancing the undercut more rapidly, but problems may arise if this allows an air gap to be formed over a large area. In this situation, the intersection of major structures, heavy blasting, and the influx of water can result in damaging air blasts (Laubscher 2003). The very favorable rate of caving follows the relation RC > RU > RD, which means that the rate of undercutting (RU) is slower than the rate of caving (RC) but faster than the rate of damage (RD) in the undercut drifts, and a very unfavorable rate of caving occurs when RC < RU < RD.

### *3.2.5 Fragmentation*

The overall success and profitability of a block caving operation will significantly depend on the fragmentation produced in the orebody during the caving process. The prediction of rock fragmentation during block caving requires understandings of the natural fragmentation of the rock mass and of the fragmentation processes that take place in the draw column. The design and operating parameters influenced by fragmentation include drawpoint size and spacing, equipment selection, draw control procedures, production rates, etc.

The degree of fragmentation of the ore occurs as a result of the caving process and influences the drawpoint spacing and design, equipment selection, and performance. The factors that affect fragmentation are as follows (Laubscher 2003):

- The in situ network of discontinuities as defined by their orientation, size, spacing, condition, and termination,
- In situ stresses and the stresses induced in the cave face or back (varying with cave height),
- Rock strengths,
- Draw column height and residence time.

The orientation of the undercut with respect to the joint sets and the direction of principal stress can have a significant effect on fragmentation. Advancing an undercut towards the principle stress will result in high abutment stresses, which will induce caving and improve the fragmentation, but could result in damage on the undercut and production levels (Laubscher 2003).

The rate of draw has an influence on the time that a block remains in the draw column, which, in turn, influences the fragmentation. A faster draw rate is assumed to result in larger rock fragments and, inversely, a low draw rate results in a better fragmentation (Brown 2007).

## 4 Establishment of the Interaction Matrix

The RES approach can be used for the analysis of coupled mechanisms in rock engineering problems (Hudson 1992). The RES uses a top-down analytic model to treat the rock mass, the boundary conditions, and the engineering activities as a complete, interactive, and dynamic system. The interactions between parameters in the RES approach are represented using an "interaction matrix", as illustrated in Fig. 6. In the interaction matrix, all factors influencing the system are arranged along the leading diagonal. The influence of each individual factor on any other factor is included at the corresponding off-diagonal position of the

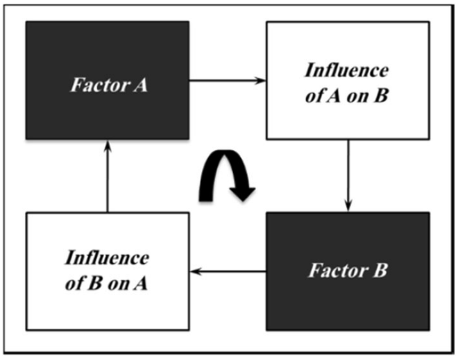


**Fig. 6** The principle of the interaction matrix (Jiao and Hudson 1995)

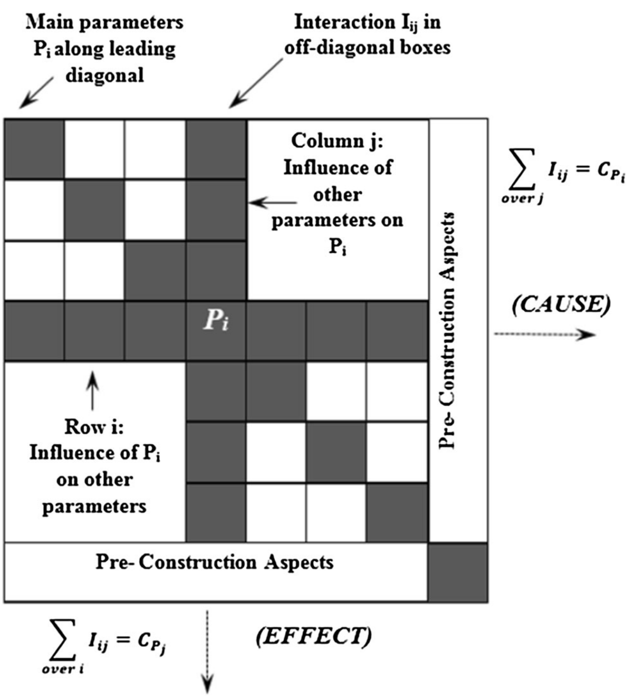


**Fig. 7** Summation of coding values in the row and column through each parameter to establish the cause and effect coordinates (Hudson 1992)

matrix, so that the (A, B)-th element represents the influence of parameter A on parameter B. In principle, there is no limitation to the number of factors that may be included in an interaction matrix.

A more common illustration of a higher-dimensional interaction matrix is shown in Fig. 7. The row passing through $P_i$ represents the influence of $P_i$ on all the other factors in the system, while the column through $P_i$ represents the influence of the other factors, or the rest of the system, on parameter $P_i$.

To quantify the importance of the interactions, a coding method is required. The most common approach is the ESQ method proposed by Hudson (1992). Typically, coding values between 0 and 4 are employed with ESQ coding schemes, as shown in Table 1.

**Table 1** Expert semi-quantitative (ESQ) coding of the parameters' interaction intensity (Hudson 1992)

| Coding | Description |
|---|---|
| 0 | No interaction |
| 1 | Weak interaction |
| 2 | Medium interaction |
| 3 | Strong interaction |
| 4 | Critical interaction |

After coding the matrix, from the matrix construction, the rows and columns of the interaction matrix are added so that each classification category represents the cause and effect of the influence on the entire system. The degree of influence of each classification category ($i$) on the entire system as a "cause" is denoted with $C_{pi}$ and as an "effect" with $E_{pi}$. $C_{pi}$ is specified on the right of each row and $E_{pi}$ is specified below each column, as illustrated in Fig. 7. The two categories can be expressed as follows:

$$C_{pi} = \sum_{j=1}^{n} a_{ij} \quad (1)$$

$$E_{pj} = \sum_{j=1}^{n} a_{ij} \quad (2)$$

The effective role of each factor is shown in the cause versus effect diagram (Fig. 8). In this figure, the diagonal of the diagram is the locus of points that have the same value. Along this diagonal and far away from the center of the coordinate system, the summation of cause and effect ($C + E$) increases. The factors located in the bottom-right portion of the diagram are "dominant" in the system. In a similar manner, the "subordinate" factors are defined as those which are highly dominated by the system and are located in the top-left corner of the diagram. The cause–effect plot is a helpful tool in understanding the behavior of each factor individually, as well as studying the whole system. For example, the points that tend to distribute perpendicularly to the $C = E$ diagonal show a low level of interactivity between factors, whereas a high interactivity will result in the points being distributed along the main diagonal line (Hudson 1992).

The ESQ method often requires a deep understanding of rock engineering and the ability to determine the relative intensity of the effects among leading diagonal terms. The user must also be an expert in rock engineering. It is well known that the bottleneck of expert systems is the gaining and representation of experts' knowledge, so this bottleneck also exists in this method (Yang and Zhang 1998). Due to the existence of uncertainties in the characterization of parameters, their relations, or even in the mechanics of

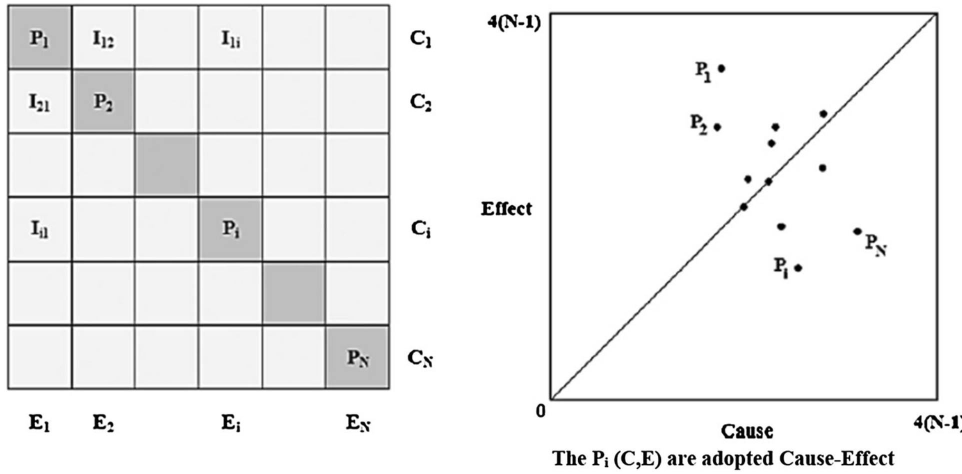


**Fig. 8** The cause–effect (*C*, *E*) plot for the supposed case comprising *N* influencing factors (Hudson 1992)

the problem, an accurate and unique code cannot be selected. The unique codes cannot, thus, fully express the correct particular interaction (Naghadehi et al. 2011).

To cope with the problem of uncertainty in the interaction matrix coding, Naghadehi et al. (2011) proposed to consider a PESQ coding method. In this method, different probability values are assigned to each interaction matrix. In other words, to each interaction, the probabilities of having one of the possible considered coding values (e.g., from 0 to 4 in this case) are assigned. This information can be represented as a set of matrices (five matrices will be employed in the case that a 0–4 coding is used), where each such matrix contains, in its $(i, j)$-th position, the probability that such a particular code represents the influence of $P_i$ on $P_j$.

We implemented the new coding (PESQ) in the RES method by forming the five interactions matrices discussed above (one for each code value of 0 to 4). These matrices are called $M_0$ to $M_4$. The 14 principal parameters are placed in the leading diagonal positions of the matrices, together with the "potential cavability" of the rock mass, which is considered as the 15th parameter of the analysis. So, based on the typical RES methodology, the column of interactions through this parameter represents how the other selected parameters affect potential cavability, while the row through the box of potential capability represents the influence of potential cavability on the selected parameters.

As previously mentioned, in the PESQ method, the probability codes are considered for each interaction coding value. So, instead of specifying a unique code value for every interaction, the probability of different values of the codes (from 0 to 4 in this case) is assigned for interactions. This can be expressed by five matrices ($M_0$–$M_4$, one for each code value from 0 to 4), where the off-diagonal elements of each matrix contain the probabilities for occurrence of that particular code for that particular interaction (Tables 2, 3, 4, 5, 6).

As an example of the coding process, the influence of joint persistence parameter ($P_6$) on the fragmentation ($P_{12}$) is explained [i.e., element (6, 12) in matrices $M_0$–$M_4$; see Tables 2, 3, 4, 5, 6]. This interaction is considered to be a "strong interaction"; thus, probabilities are assigned 0 % for the occurrence of code 0 (no interaction), 5 % for the occurrence of code 1 (weak interaction), 10 % for the occurrence of code 2 (medium interaction), 65 % for the occurrence of code 3 (strong interaction), and 20 % for the occurrence of code 4 (critical interaction). It is worth mentioning that the PESQ is somehow subjective, but it has the advantage that it allows us to incorporate our best estimates of uncertainties into the analysis.

## 5 Results

As explained in the previous section, in the coding of the interaction matrix using a conventional method (ESQ), the effect of each parameter on the system, as well as the effect of the system on the each parameter, can be calculated (respectively) as the sum of the codes in the parameter's row and column within the interaction matrix.

In the PESQ coding method, the code probabilities are in the off-diagonal elements of the matrix, which means that, in this method, instead of unique $C_i$ and $E_i$ values, the probability distributions of $C_i$ and $E_i$ parameters can be calculated. Also, when the distributions are known, the expected values of $C_i$ and $E_i$ for each parameter ($P_i$) can be computed.

Since we have 15 parameters in the interaction matrix, the corresponding cause or effect for any parameter is the sum of 14 different interaction values. As the array element $a_{ij}$ is considered to be the effect of the $i$-th parameter on parameter $j$, one can write:

**Table 2** Interaction matrix $M_0$ for the probabilities of code 0 for cavability

| | | | | | | | | | | | | | | |
|---|---|---|---|---|---|---|---|---|---|---|---|---|---|---|
| **$P_1$** | 5 | 5 | 20 | 20 | 0 | 0 | 80 | 90 | 10 | 0 | 0 | 5 | 0 | 5 |
| 15 | **$P_2$** | 5 | 0 | 0 | 0 | 0 | 60 | 5 | 0 | 0 | 0 | 10 | 0 | 0 |
| 60 | 5 | **$P_3$** | 70 | 10 | 5 | 15 | 100 | 10 | 0 | 0 | 0 | 10 | 5 | 0 |
| 90 | 5 | 35 | **$P_4$** | 35 | 35 | 35 | 70 | 5 | 5 | 0 | 0 | 10 | 0 | 0 |
| 100 | 5 | 35 | 100 | **$P_5$** | 5 | 5 | 0 | 0 | 5 | 0 | 5 | 30 | 30 | 0 |
| 100 | 5 | 15 | 100 | 15 | **$P_6$** | 25 | 5 | 5 | 0 | 0 | 0 | 10 | 20 | 0 |
| 100 | 25 | 20 | 100 | 5 | 5 | **$P_7$** | 5 | 15 | 0 | 0 | 0 | 5 | 10 | 0 |
| 100 | 100 | 100 | 100 | 5 | 70 | 0 | **$P_8$** | 5 | 5 | 0 | 0 | 65 | 100 | 0 |
| 5 | 5 | 100 | 100 | 20 | 10 | 0 | 5 | **$P_9$** | 0 | 0 | 0 | 20 | 25 | 0 |
| 100 | 5 | 20 | 90 | 5 | 5 | 90 | 100 | 80 | **$P_{10}$** | 0 | 0 | 5 | 20 | 0 |
| 100 | 5 | 15 | 80 | 5 | 10 | 75 | 100 | 100 | 35 | **$P_{11}$** | 0 | 5 | 25 | 0 |
| 100 | 90 | 80 | 100 | 100 | 85 | 100 | 100 | 100 | 100 | 5 | **$P_{12}$** | 20 | 25 | 0 |
| 100 | 0 | 15 | 50 | 5 | 10 | 5 | 90 | 90 | 5 | 0 | 0 | **$P_{13}$** | 0 | 0 |
| 100 | 70 | 80 | 95 | 35 | 55 | 70 | 100 | 80 | 5 | 0 | 0 | 90 | **$P_{14}$** | 0 |
| 100 | 100 | 100 | 100 | 100 | 100 | 100 | 100 | 100 | 100 | 100 | 100 | 100 | 100 | **$P_{15}$** |

$P_1$ UCS, $P_2$ in situ stress, $P_3$ joint spacing, $P_4$ joint orientation, $P_5$ joint aperture, $P_6$ joint persistence, $P_7$ joint roughness, $P_8$ joint filling, $P_9$ water, $P_{10}$ hydraulic radius, $P_{11}$ caving rate, $P_{12}$ fragmentation, $P_{13}$ block height, $P_{14}$ undercut direction, $P_{15}$ potential of cavability

**Table 3** Interaction matrix $M_1$ for the probabilities of code 1 for cavability

| | | | | | | | | | | | | | | |
|---|---|---|---|---|---|---|---|---|---|---|---|---|---|---|
| **$P_1$** | 20 | 25 | 65 | 75 | 15 | 5 | 15 | 10 | 70 | 5 | 0 | 70 | 5 | 10 |
| 70 | **$P_2$** | 15 | 0 | 5 | 5 | 5 | 25 | 10 | 0 | 0 | 5 | 65 | 0 | 0 |
| 25 | 55 | **$P_3$** | 25 | 40 | 35 | 70 | 0 | 70 | 10 | 0 | 0 | 30 | 20 | 0 |
| 10 | 20 | 50 | **$P_4$** | 55 | 55 | 55 | 25 | 15 | 10 | 5 | 5 | 65 | 5 | 0 |
| 0 | 10 | 50 | 0 | **$P_5$** | 20 | 5 | 5 | 0 | 5 | 5 | 5 | 60 | 60 | 10 |
| 0 | 20 | 50 | 0 | 50 | **$P_6$** | 70 | 15 | 5 | 5 | 5 | 5 | 55 | 60 | 0 |
| 0 | 60 | 65 | 0 | 25 | 25 | **$P_7$** | 10 | 80 | 5 | 5 | 5 | 25 | 80 | 0 |
| 0 | 0 | 0 | 0 | 10 | 15 | 5 | **$P_8$** | 10 | 10 | 5 | 5 | 20 | 0 | 0 |
| 15 | 15 | 0 | 0 | 60 | 50 | 10 | 5 | **$P_9$** | 5 | 5 | 10 | 65 | 70 | 0 |
| 0 | 20 | 50 | 10 | 15 | 25 | 10 | 0 | 15 | **$P_{10}$** | 0 | 0 | 10 | 70 | 0 |
| 0 | 15 | 50 | 15 | 15 | 20 | 15 | 0 | 0 | 50 | **$P_{11}$** | 0 | 10 | 60 | 0 |
| 0 | 10 | 20 | 0 | 0 | 15 | 0 | 0 | 0 | 0 | 15 | **$P_{12}$** | 65 | 60 | 0 |
| 0 | 0 | 55 | 30 | 10 | 15 | 10 | 10 | 10 | 20 | 5 | 5 | **$P_{13}$** | 5 | 5 |
| 0 | 20 | 15 | 5 | 50 | 35 | 30 | 0 | 20 | 70 | 5 | 0 | 10 | **$P_{14}$** | 0 |
| 0 | 0 | 0 | 0 | 0 | 0 | 0 | 0 | 0 | 0 | 0 | 0 | 0 | 0 | **$P_{15}$** |

$P_1$ UCS, $P_2$ in situ stress, $P_3$ joint spacing, $P_4$ joint orientation, $P_5$ joint aperture, $P_6$ joint persistence, $P_7$ joint roughness, $P_8$ joint filling, $P_9$ water, $P_{10}$ hydraulic radius, $P_{11}$ caving rate, $P_{12}$ fragmentation, $P_{13}$ block height, $P_{14}$ undercut direction, $P_{15}$ potential of cavability

**Table 4** Interaction matrix $M_2$ for the probabilities of code 2 for cavability

| | | | | | | | | | | | | | | |
|---|---|---|---|---|---|---|---|---|---|---|---|---|---|---|
| **$P_1$** | 60 | 50 | 10 | 5 | 65 | 15 | 5 | 0 | 15 | 50 | 10 | 15 | 15 | 40 |
| 10 | **$P_2$** | 20 | 10 | 15 | 15 | 10 | 10 | 70 | 10 | 10 | 20 | 15 | 10 | 0 |
| 10 | 25 | **$P_3$** | 5 | 45 | 55 | 10 | 0 | 15 | 30 | 10 | 10 | 45 | 60 | 0 |
| 0 | 55 | 10 | **$P_4$** | 10 | 10 | 10 | 5 | 65 | 50 | 15 | 10 | 15 | 40 | 0 |
| 0 | 30 | 10 | 0 | **$P_5$** | 60 | 10 | 10 | 10 | 15 | 10 | 60 | 10 | 10 | 70 |
| 0 | 55 | 20 | 0 | 20 | **$P_6$** | 5 | 60 | 25 | 15 | 10 | 10 | 20 | 10 | 75 |
| 0 | 10 | 10 | 0 | 55 | 55 | **$P_7$** | 15 | 5 | 10 | 10 | 15 | 60 | 10 | 10 |
| 0 | 0 | 0 | 0 | 15 | 10 | 10 | **$P_8$** | 65 | 60 | 15 | 15 | 10 | 0 | 5 |
| 50 | 50 | 0 | 0 | 15 | 35 | 25 | 10 | **$P_9$** | 30 | 30 | 50 | 10 | 5 | 90 |
| 0 | 60 | 15 | 0 | 65 | 55 | 0 | 0 | 5 | **$P_{10}$** | 10 | 5 | 50 | 10 | 0 |
| 0 | 55 | 20 | 5 | 55 | 50 | 10 | 0 | 0 | 15 | **$P_{11}$** | 5 | 50 | 15 | 10 |
| 0 | 0 | 0 | 0 | 0 | 0 | 0 | 0 | 0 | 0 | 50 | **$P_{12}$** | 10 | 10 | 0 |
| 0 | 10 | 20 | 15 | 50 | 50 | 50 | 0 | 0 | 55 | 20 | 10 | **$P_{13}$** | 10 | 40 |
| 0 | 10 | 5 | 0 | 15 | 10 | 0 | 0 | 0 | 15 | 10 | 10 | 0 | **$P_{14}$** | 10 |
| 0 | 0 | 0 | 0 | 0 | 0 | 0 | 0 | 0 | 0 | 0 | 0 | 0 | 0 | **$P_{15}$** |

$P_1$ UCS, $P_2$ in situ stress, $P_3$ joint spacing, $P_4$ joint orientation, $P_5$ joint aperture, $P_6$ joint persistence, $P_7$ joint roughness, $P_8$ joint filling, $P_9$ water, $P_{10}$ hydraulic radius, $P_{11}$ caving rate, $P_{12}$ fragmentation, $P_{13}$ block height, $P_{14}$ undercut direction, $P_{15}$ potential of cavability

**Table 5** Interaction matrix $M_3$ for the probabilities of code 3 for cavability

| | | | | | | | | | | | | | | |
|---|---|---|---|---|---|---|---|---|---|---|---|---|---|---|
| **$P_1$** | 10 | 15 | 5 | 0 | 15 | 70 | 0 | 0 | 5 | 40 | 60 | 5 | 50 | 30 |
| 5 | **$P_2$** | 45 | 70 | 45 | 45 | 55 | 5 | 10 | 50 | 55 | 50 | 5 | 50 | 10 |
| 5 | 10 | **$P_3$** | 0 | 5 | 5 | 5 | 0 | 5 | 50 | 70 | 20 | 10 | 10 | 80 |
| 0 | 15 | 5 | **$P_4$** | 0 | 0 | 0 | 0 | 10 | 25 | 60 | 45 | 5 | 45 | 20 |
| 0 | 50 | 5 | 0 | **$P_5$** | 10 | 60 | 60 | 50 | 60 | 65 | 20 | 0 | 0 | 20 |
| 0 | 15 | 10 | 0 | 10 | **$P_6$** | 0 | 15 | 55 | 60 | 65 | 65 | 10 | 5 | 20 |
| 0 | 5 | 5 | 0 | 10 | 10 | **$P_7$** | 55 | 0 | 65 | 65 | 55 | 10 | 0 | 80 |
| 0 | 0 | 0 | 0 | 50 | 5 | 25 | **$P_8$** | 15 | 20 | 60 | 30 | 5 | 0 | 80 |
| 25 | 20 | 0 | 0 | 5 | 5 | 50 | 65 | **$P_9$** | 50 | 50 | 35 | 5 | 0 | 10 |
| 0 | 10 | 10 | 0 | 10 | 10 | 0 | 0 | 0 | **$P_{10}$** | 25 | 80 | 25 | 0 | 0 |
| 0 | 20 | 10 | 0 | 20 | 15 | 0 | 0 | 0 | 0 | **$P_{11}$** | 70 | 25 | 0 | 70 |
| 0 | 0 | 0 | 0 | 0 | 0 | 0 | 0 | 0 | 0 | 20 | **$P_{12}$** | 5 | 5 | 0 |
| 0 | 30 | 10 | 5 | 20 | 20 | 20 | 0 | 0 | 15 | 65 | 25 | **$P_{13}$** | 70 | 50 |
| 0 | 0 | 0 | 0 | 0 | 0 | 0 | 0 | 0 | 10 | 60 | 60 | 0 | **$P_{14}$** | 70 |
| 0 | 0 | 0 | 0 | 0 | 0 | 0 | 0 | 0 | 0 | 0 | 0 | 0 | 0 | **$P_{15}$** |

$P_1$ UCS, $P_2$ in situ stress, $P_3$ joint spacing, $P_4$ joint orientation, $P_5$ joint aperture, $P_6$ joint persistence, $P_7$ joint roughness, $P_8$ joint filling, $P_9$ water, $P_{10}$ hydraulic radius, $P_{11}$ caving rate, $P_{12}$ fragmentation, $P_{13}$ block height, $P_{14}$ undercut direction, $P_{15}$ potential of cavability

**Table 6** Interaction matrix $M_4$ for the probabilities of code 4 for cavability

| | | | | | | | | | | | | | | |
|---|---|---|---|---|---|---|---|---|---|---|---|---|---|---|
| **$P_1$** | 5 | 5 | 0 | 0 | 5 | 10 | 0 | 0 | 0 | 5 | 30 | 5 | 30 | 15 |
| 0 | **$P_2$** | 15 | 20 | 35 | 35 | 30 | 0 | 5 | 40 | 35 | 25 | 5 | 40 | 90 |
| 0 | 5 | **$P_3$** | 0 | 0 | 0 | 0 | 0 | 0 | 10 | 20 | 70 | 5 | 5 | 20 |
| 0 | 5 | 0 | **$P_4$** | 0 | 0 | 0 | 0 | 5 | 10 | 20 | 40 | 5 | 10 | 80 |
| 0 | 5 | 0 | 0 | **$P_5$** | 5 | 20 | 25 | 40 | 15 | 20 | 10 | 0 | 0 | 0 |
| 0 | 5 | 5 | 0 | 5 | **$P_6$** | 0 | 5 | 10 | 20 | 20 | 20 | 5 | 5 | 5 |
| 0 | 0 | 0 | 0 | 5 | 5 | **$P_7$** | 15 | 0 | 20 | 20 | 25 | 0 | 0 | 10 |
| 0 | 0 | 0 | 0 | 20 | 0 | 60 | **$P_8$** | 5 | 5 | 20 | 50 | 0 | 0 | 15 |
| 5 | 10 | 0 | 0 | 0 | 0 | 15 | 15 | **$P_9$** | 15 | 15 | 5 | 0 | 0 | 0 |
| 0 | 5 | 5 | 0 | 5 | 5 | 0 | 0 | 0 | **$P_{10}$** | 65 | 15 | 10 | 0 | 100 |
| 0 | 5 | 5 | 0 | 5 | 5 | 0 | 0 | 0 | 0 | **$P_{11}$** | 25 | 10 | 0 | 10 |
| 0 | 0 | 0 | 0 | 0 | 0 | 0 | 0 | 0 | 0 | 10 | **$P_{12}$** | 0 | 0 | 100 |
| 0 | 60 | 0 | 0 | 15 | 5 | 15 | 0 | 0 | 5 | 10 | 60 | **$P_{13}$** | 15 | 5 |
| 0 | 0 | 0 | 0 | 0 | 0 | 0 | 0 | 0 | 0 | 25 | 30 | 0 | **$P_{14}$** | 20 |
| 0 | 0 | 0 | 0 | 0 | 0 | 0 | 0 | 0 | 0 | 0 | 0 | 0 | 0 | **$P_{15}$** |

$P_1$ UCS, $P_2$ in situ stress, $P_3$ joint spacing, $P_4$ joint orientation, $P_5$ joint aperture, $P_6$ joint persistence, $P_7$ joint roughness, $P_8$ joint filling, $P_9$ water, $P_{10}$ hydraulic radius, $P_{11}$ caving rate, $P_{12}$ fragmentation, $P_{13}$ block height, $P_{14}$ undercut direction, $P_{15}$ potential of cavability

$$C_i = \sum_{j=1, j\neq i}^{15} a_{ij} \tag{3}$$

$$E_i = \sum_{j=1, j\neq i}^{15} a_{ji} \tag{4}$$

where $a_{ij}$ can have any integer value $k \in \{0, 1, 2, 3, 4\}$ with a defined probability, which is considered in the matrices (Tables 2, 3, 4, 5, 6). Hence, for any parameter, the probability of the cause or effect having a determined value $S$ ($0 \leq S \leq 60$, note that there are 15 non-diagonal positions in each row and column with values 0 to 4, $C_i$ and $E_i$ will, thus, be between 0 and 60) is the sum of all probable states in which the sum of $k_i$ is equal to $S$. In other words, it can be written as:

$$P_r(C_i == S) = \sum_{k_1+k_2+\cdots+k_{15}=S} \prod_{j=1, j\neq i}^{15} P_r(a_{ij} == k_j) \tag{5}$$

$$P_r(E_i == S) = \sum_{k_1+k_2+\cdots+k_{15}=S} \prod_{j=1, j\neq i}^{15} P_r(a_{ij} == k_j) \tag{6}$$

where $C_i$ and $E_i$ are, respectively, the values of the cause and effect of parameter $I$ and $P_r = (p == q)$ is the probability of $p$ being equal to $q$ and $k_j \in \{0, 1, 2, 3, 4\}$. Figure 9 shows the probability distributions for parameters $P_5$ and $P_{12}$.

As an example, Fig. 9 for parameter $P_{12}$ shows the probability distributions for the cause and effect of the "fragmentation" parameter. As can be seen, the value of $C_{12}$ would be between 6 and 12 with a probability of more

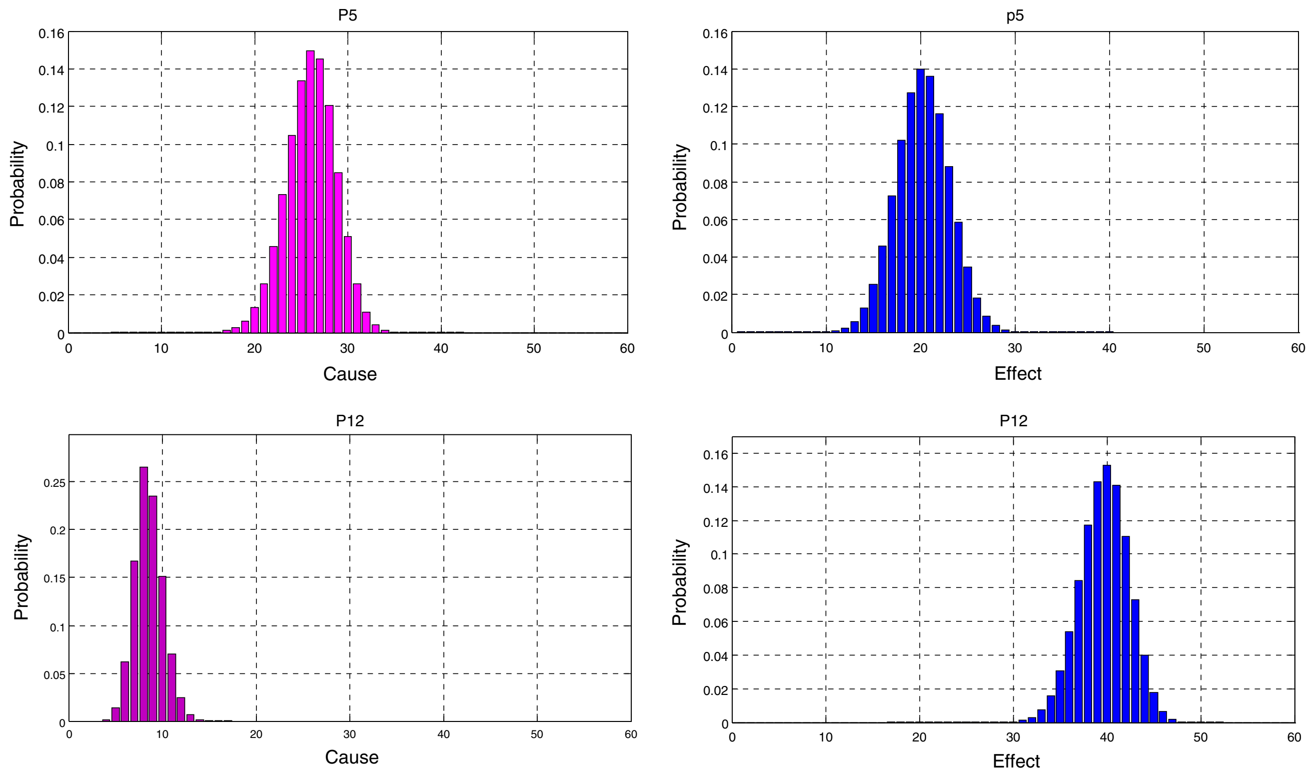


**Fig. 9** Probability mass distributions for the cause and effect of $P_5$ and $P_{12}$

than 60 % and, similarly, the value of $E_{12}$ would be between 35 and 43 with a probability higher than 50 % (similar graphs can be plotted for all the parameters).

In addition, by combining the probability distributions of $C_i$ and $E_i$ for each parameter ($P_i$), probabilistic ($C$, $E$) plots can also be produced. Figures 10 and 11 show these plots for the UCS parameter ($P_1$) and the block height parameter ($P_{13}$).

The probabilistic ($C$, $E$) plots presented in Figs. 10 and 11 can be analyzed similar to the conventional deterministic ($C$, $E$) plot presented in Fig. 8. As previously mentioned, the deterministic interaction intensity and dominance of each parameter in the system can be analyzed according to its position in the ($C$, $E$) plot. Similarly, the probabilities of interaction intensity and dominance can be calculated by using the probabilistic ($C$, $E$) plots.

For some parameters, being further away from the diagonal line with equation $C = E$ (the probability content is in the lower-right region) indicates that they have a high dominance on the system. When the probability content is in the upper-left region, this indicates that the system has a dominance on them, and, finally, the parameters are neutral with respect to the system when the probability content is mainly on the $C = E$ line. Figure 12 shows the cause–effect diagram plotted using the accepted values of cause and effect of parameters.

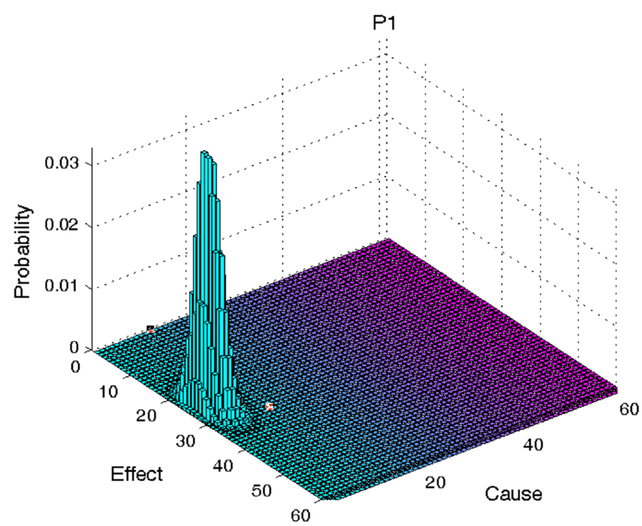


**Fig. 10** ($C$, $E$) plot for the uniaxial compressive strength (UCS) ($P_1$) parameter in the system

Furthermore, the probabilistic ($C$, $E$) plots allow us to identify the importance of parameters and their influence on the system. For this reason, the probability distribution of $C + E$ and $C - E$ values for all parameters can be calculated. The results for parameters $P_5$ and $P_{12}$ are shown in Figs. 13 and 14, respectively (similar graphs can be plotted for all the parameters).

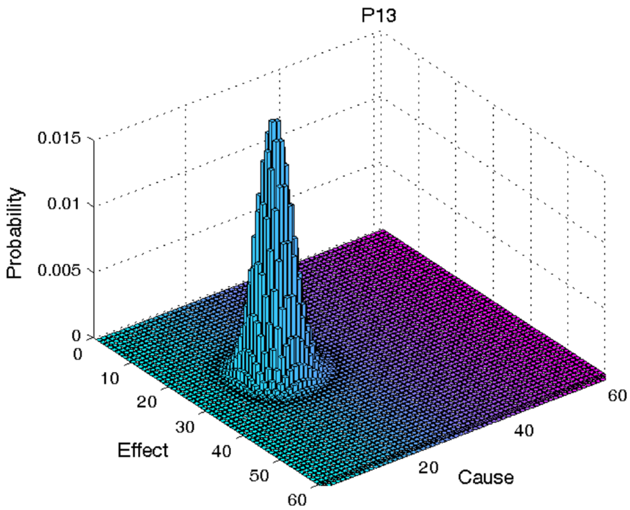


**Fig. 11** ($C$, $E$) plot for the block height ($P_{13}$) parameter in the system

From the results of Figs. 13 and 14, the expected interaction intensities ($C + E$) and expected dominance ($C - E$) for any parameter can be plotted (Figs. 15 and 16). In these figures, the error bars, which show the uncertainty estimates, are calculated using the standard deviation values.

The results of Figs. 12, 15, and 16 indicate that almost all 14 main parameters are rather interactive and have a significant influence on the "outcome" parameter (i.e., potential cavability); therefore, they should be taken into account in engineering decisions.

Based on the cause–effect probabilistic diagram of the 15 parameters, the following points are noteworthy:

- All parameters considered in the cavability system are rather interactive because the probability of their position is higher along the diagonal of the $C$–$E$ diagram.
- Parameter $P_2$ has a higher probability of being interactive, while the lowest probability of being interactive belongs to $P_1$ and $P_4$.
- The UCS ($P_1$) and the in situ stress ($P_2$) are the parameters that have the highest probability to dominate the system, while the fragmentation ($P_{12}$) and the potential cavability ($P_{15}$) are the parameters which have the highest probability of being dominated by the system.

## 6 Conclusion

The cavability of the deposit is a fundamental feature of mine design. Initiating the cave and then sustaining the cave throughout the mine's life are critical for achieving the desired productivity and, thus, directly impact the economics of the project.

Many parameters influence the rock mass cavability in block caving mines, which are divided into two categories: natural parameters and induced parameters. Understanding the influence and importance of these parameters has an important role in investigating and predicting the cavability in block caving mines. For this reason, the rock engineering system (RES) method has been used in this study. In this method, simultaneous assessment of all parameters and their impact on the cavability of rock mass is possible. As the interaction matrix codes are not unique in this method, the probabilistic coding, the other typical RES procedure, can non-deterministically be performed to allow consideration of uncertainties in the RES method.

The probabilistic RES approach allows identifying the parameters with the highest probability of being dominant or subordinate, and also the parameters with the highest probability of being interactive. That is, variability and/or uncertainties can be explicitly included in the analysis, and the effects of such uncertainties can be quantified. Such information is important in practice, for example, in the fieldwork; a designer can identify parameters that should be characterized in more detail. For instance, our results showed that the parameter related to the existence of "in situ stress" ($P_2$) has the highest expected interaction

**Fig. 12** Cause–effect diagram based on the accepted values of the cause and effect of parameters

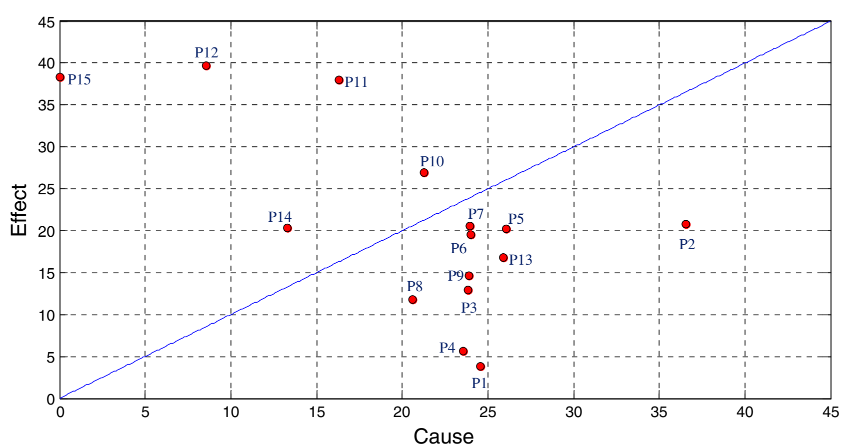

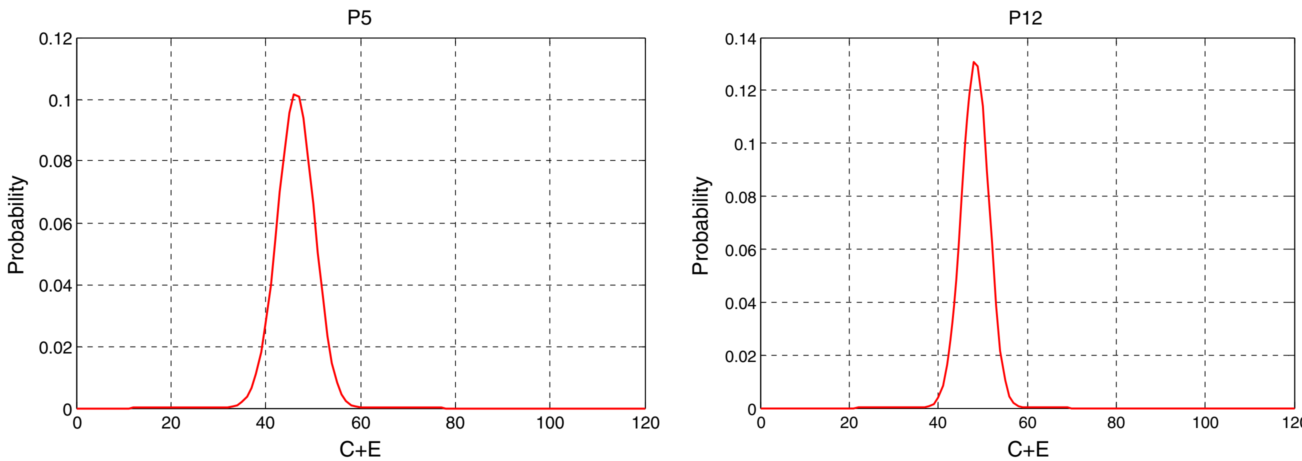


**Fig. 13** Probability distribution of $C + E$ values for the $P_5$ and $P_{12}$ parameters

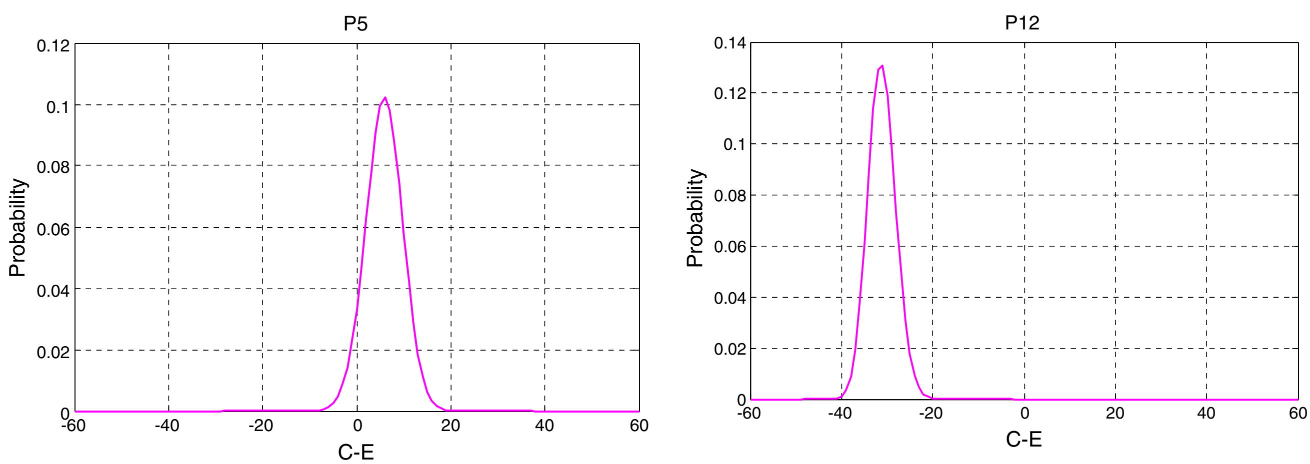


**Fig. 14** Probability distribution of $C - E$ values for the $P_5$ and $P_{12}$ parameters

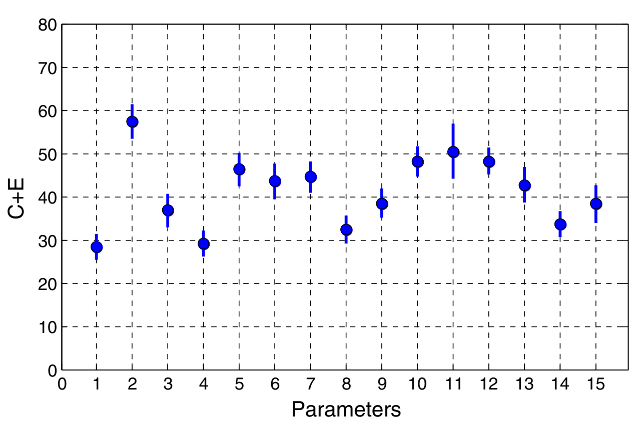


**Fig. 15** Mean values and standard deviation limits for the interactivity of 15 parameters affecting the cavability of rock mass

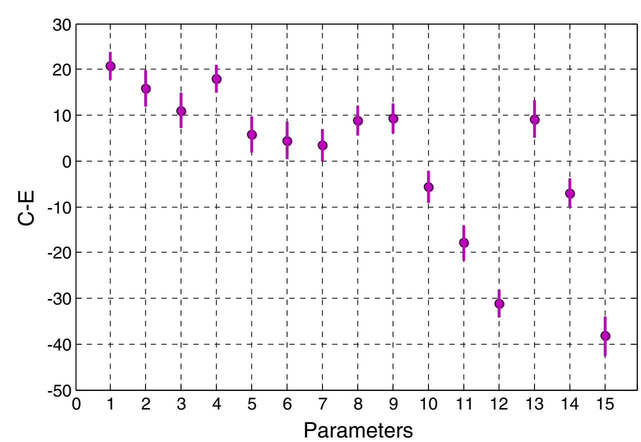


**Fig. 16** Mean values and standard deviation limits for the subordinance of 15 parameters affecting the cavability of rock mass

with the system (in other words, it is the most important parameter), therefore suggesting the orientation and magnitude of in situ stress to be accurately measured in field surveys. Similarly, the “caving rate”, “fragmentation”, and “joint aperture” have also been found to be quite significant parameters.

In addition, the probabilistic RES methodology permits to compute the uncertainties of computed results. For example, we observed that the "caving rate" parameter has the largest standard deviation (hence, the greater uncertainty) among all the parameters. Similar comments could be made about the dominance/subordinance of the system. Such information could not be obtained by using only a deterministic approach and/or mean values.

## References

Brady BHG, Brown ET (2004) Rock mechanics for underground mining. Springer, New York

Brown ET (2007) Block caving geomechanics. International Caving Study 1997–2004. Julius Kruttschnitt Mineral Research Centre, The University of Queensland

Budetta P, Santo A, Vivenzio F (2008) Landslide hazard mapping along the coastline of the Cilento region (Italy) by means of a GIS-based parameter rating approach. Geomorphology 94(3):340–352

Butcher RJ (2000) Block cave undercutting—aims, strategies, methods and management. Proc MassMin 2000:405–411

Diering JAC, Laubscher DH (1987) Practical approach to the numerical stress analysis of mass mining operations. Institution of Mining and Metallurgy Transactions, Section A: Mining Industry, vol 96

Heslop TG, Laubscher DH (1981) Draw control in caving operations on Southern African chrysotile asbestos mines. Design and operation of caving and sublevel stoping mines, pp 775–774

Hudson JA (1992) Rock engineering systems, theory and practice. Ellis Horwood, Chichester

Hudson JA, Harrison JP (1992) A new approach to studying complete rock engineering problems. Quart J Eng Geol Hydrogeol 25(2):93–105

Jiao Y, Hudson JA (1995) The fully-coupled model for rock engineering systems. Int J Rock Mech Min Sci Geomech Abs 32:491–512

Jiao Y, Hudson JA (1998) Identifying the critical mechanisms for rock engineering design. Geotechnique 48(3):319–335

Julian DE (1974) Future developments in block caving. Skillings Mining Review, pp 12–15

Kendorski FS (1978) Cavability of ore deposits. Min Eng 30:628-631

Laubscher DH (1990) A geomechanics classification system for the rating of rock mass in mine design. J S Afr Inst Metall 90(10):267–273

Laubscher DH (1994) Cave mining—the state of the art. J S Afr Inst Min Metall 94(10):2279

Laubscher D (2000a) A practical guide manual on block caving. International Caving Study (1997–2000). Capitulo, pp 1–3

Laubscher DH (2000b) A practical manual on block caving. Julius Kruttschnitt Mineral Research Centre, Brisbane

Laubscher DH (2003) Cave mining handbook. De Beers, Johannesburg

Lorig LJ, Board MP, Potyondy DO, Coetzee MJ (1995) Numerical modelling of caving using continuum and micro-mechanical models. In: Proceedings of CAMr95: 3rd Canadian conference on computer applications in the minerals Industry, Montreal, Quebec, Canada, October 1995

Mahtab MA, Dixon JD (1976) Influence of rock fractures and block boundary weakening on cavability. Trans Soc Min Eng AIME 260:6–12

Mawdesley C (2002) Predicting rock mass cavability in block caving mines. Ph.D. thesis, University of Queensland

Mawdesley C, Trueman R, Whiten W (2001) Extending the Mathews stability graph for open-stope design. Transactions of the Institution of Mining and Metallurgy, Mining Technology, Section A, pp 27–39

Obert L, Munson R, Rich C (1976) Caving properties of the Climax ore body. Trans Soc Min Eng AIME 260:129–133

Rozos D, Pyrgiotis L, Skias S, Tsagaratos P (2008) An implementation of rock engineering system for ranking the instability potential of natural slopes in Greek territory. An application in Karditsa County. Landslides 5(3):261–270

Sainsbury B-A (2012) A model for cave propagation and subsidence assessment in jointed rock masses. Doctoral dissertation, the University of New South Wales

Shang YJ, Wang SJ, Li GC, Yang ZF (2000) Retrospective case example using a comprehensive suitability index (CSI) for siting the Shisan-Ling power station, China. Int J Rock Mech Min Sci 37(5):839–853

van As A, Jeffrey RG (2000) Hydraulic fracturing as a cave inducement technique at Northparkes Mines. Proc MassMin 2000:165–172

White DH (1977) Predicting fragmentation characteristics of a block caving orebody. M.Sc. thesis, University of Arizona

Yang Y-J, Zhang Q (1998) The application of neural networks to rock engineering systems (RES). Int J Rock Mech Min Sci 35(6):727–745

Younessi A, Rasouli V (2010) A fracture sliding potential index for wellbore stability analysis. Int J Rock Mech Min Sci 47(6):927–939

Zare Naghadehi M, Jimenez R, KhaloKakaie R, Jalali S-ME (2011) A probabilistic systems methodology to analyze the importance of factors affecting the stability of rock slopes. Eng Geol 118(3):82–92

Zare Naghadehi M, Jimenez R, KhaloKakaie R, Jalali S-ME (2013) A new open-pit mine slope instability index defined using the improved rock engineering systems approach. Int J Rock Mech Min Sci 61:1–14

Zhang LQ, Yang ZF, Liao QL, Chen J (2004) An application of the rock engineering systems (RES) methodology in rockfall hazard assessment on the Chengdu-Lhasa Highway, China. Int J Rock Mech Min Sci 41:833–838